JOURNAL OF MATERIALS SCIENCE 23 (1988) 3480–3484

# Iron precipitation in Cu–Au–Fe alloys

D. K-H. FINKLER*‡, T. HECK‡, A. E. MAURER*‡, S. J. CAMPBELL*, U. GONSER‡
*Department of Physics, University College, University of New South Wales, Australian Defence Force Academy, Campbell, ACT 2600, Australia
‡Angewandte Physik, Universität des Saarlandes, D-6600 Saarbrücken, FRG

Interest is focused on the segregation and clustering behaviour of iron atoms in fcc $Cu_{100-x-y}Au_xFe_y$ alloys ($x$ = 6 to 50.7 at%, $y$ = 0.2 to 1.0 at%) of three different metallurgical states: as-rolled, fast-quenched and melt-spun. The gold concentration was varied to assess the effect of change in lattice parameter. Mössbauer spectroscopy has been used to examine iron clusters and phases in samples as functions of annealing temperature and time. The development of fcc $\gamma$-Fe, segregates with increasing annealing time at temperatures around 410° C has been monitored and the Néel temperature of the antiferromagnetic $\gamma$-Fe precipitates as well as their particle size determined, the latter by transmission electron microscopy. The increase in isomer shift with increasing gold concentration is accounted for mainly by changes in atomic volume.

## 1. Introduction

The aim of this project is to examine clustering effects and the pre-precipitation stages of impurity atoms in solid solution leading to the onset of full precipitation. Knowledge of solubility limits in alloys is, of course, of great practical significance, particularly in such areas as the commercial strengthening of non-ferrous alloys (especially aluminium and magnesium alloys [1, 2]) by precipitation-hardening. Questions such as the nucleation of precipitates and the kinetics of precipitation are however difficult to solve in specific alloys of commercial importance [3] and, because of this, the relatively straightforward fcc Cu–Au–Fe system has been selected for investigation of the early stages of precipitation. Given that the iron solubility in copper is limited [4] and that clustering effects are known to occur in Cu–Fe (e.g. [5]), the fcc Cu–Au matrix offers a convenient host both for increasing the solubility of iron (gold exhibits an extended solubility of iron [4]) and also for varying the lattice parameter of the fcc Cu–Au matrix. With suitable heat treatment, fcc $\gamma$-Fe forms metastable precipitates in a coherent fcc matrix before the formation of ferromagnetic bcc $\alpha$-Fe [6].

A comparison of the clustering and segregation behaviour of iron (0.2 to 1.0 at %) in Cu–Au alloys of three different metallurgical states, as-rolled (AR), fast-quenched (FQ) and melt-spun (MS), has been undertaken using Mössbauer spectroscopy and transmission electron microscopy (TEM) to probe the local atomic environment, particularly that of the iron atoms. The three states AR, FQ and MS have been chosen to simulate typical metallurgical conditions such as a cold-worked and distorted state, an atomically disordered state, and the influence of a fast cooling rate. The growth of coherent fcc $\gamma$-Fe precipitates as the limit of iron clusters in the fcc matrix has been monitored as a function of annealing time. This behaviour has been explored fully for Cu–Fe (e.g. [7]), but not for a ternary system such as Cu–Au–Fe.

## 2. Experimental procedure

The $Cu_{100-x-y}Au_xFe_y$ alloys ($x$ = 6, 12, 37, 50.7 at %; $y$ = 0.2 to 1 at %) were prepared as described previously [8]. Specimens in the fast-quenched state were first cold-rolled to foils with optimal thickness for the Mössbauer transmission experiments (as-rolled state) and then heat-treated at 850° C for 24 h followed by a fast quenching into ice water. The annealing temperature of 850° C was sufficiently high to ensure that the Cu–Au matrix was in an atomically disordered state [4]. Specimens in the melt-spun state of typical thickness $\sim 20\,\mu m$ were produced by the ribbon spinning technique using a copper wheel. The Mössbauer measurements (4.2 to 300 K) were carried out in a standard transmission geometry and the spectra were calibrated with respect to the centre of a room-temperature $\alpha$-Fe spectrum.

The TEM investigations were carried out in a Jeol JEM-200CX electron microscope operating at 200 kV. The JEM-200CX's cool-beam gun leads to minimal specimen damage, and the high vacuum of $10^{-5}$ Pa in the specimen area minimizes secondary damage due to ions, secondary electrons etc. Thin foils were prepared by ion-beam etching [9, 10] using a MIM IV apparatus (Kontron GmbH). A thinning rate of $\sim 1\,\mu m\,h^{-1}$ was obtained by using an acceleration voltage of 5 kV, an etching current of 20 $\mu$A and an angle between specimen surface and the argon ion beam of 12°. These conditions ensured a specimen temperature below 100° C and therefore negligible beam damage. This sample preparation technique proved to be a suitable thinning method for Cu–Au–Fe alloys, whereas attempts to prepare specimens by electro-


0022–2461/88 $03.00 + .12 

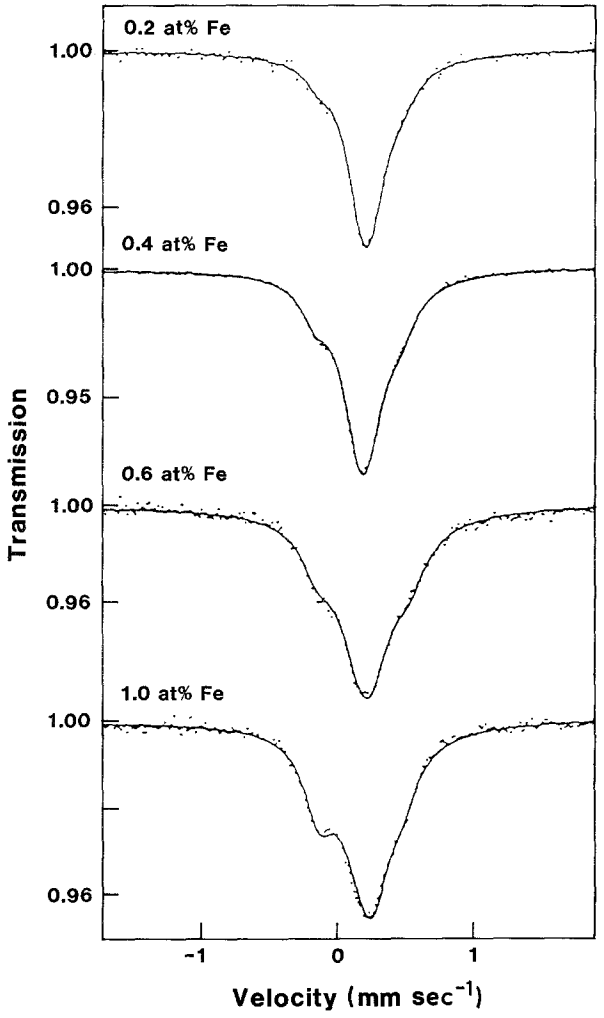


*Figure 1* Room-temperature Mössbauer spectra of $Cu_{94-y}Au_6Fe_y$ alloys in the FQ state. The full lines represent fits to the data as described in the text.

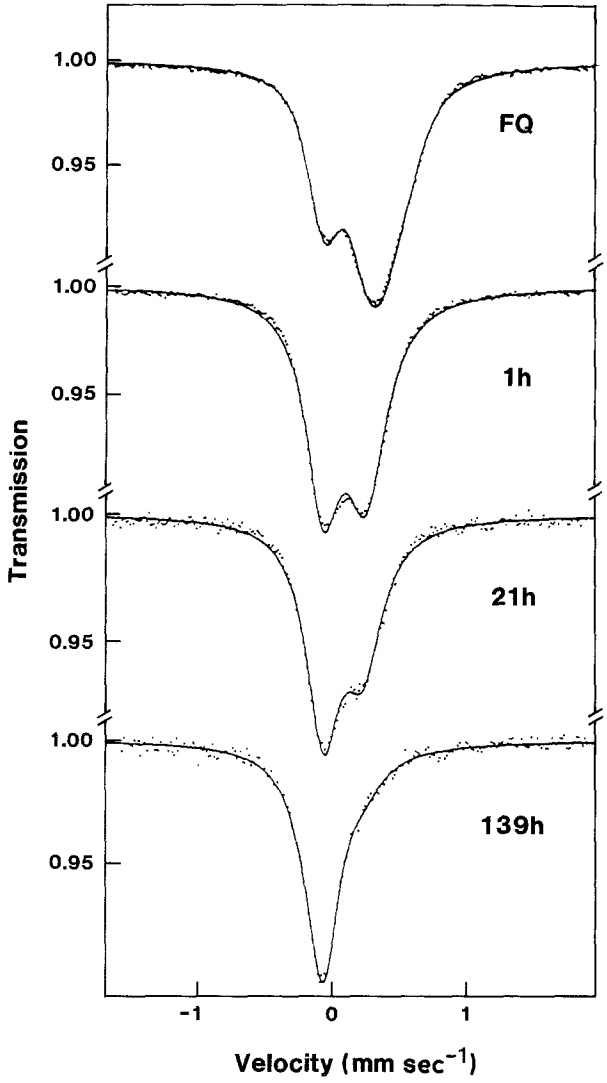


*Figure 3* Room-temperature Mössbauer spectra of the $Cu_{87}Au_{12}Fe$ FQ specimen following heat treatment at 410° C for different annealing times.

chemical polishing with the electrolyte (30% $HNO_3$, 70% $CH_3OH$) and platinum electrode used for copper and copper-based alloys [11] led to oxidation.

## 3. Results and discussion

### 3.1. Mössbauer spectroscopy

Fig. 1 shows the room-temperature Mössbauer spectra of $Cu_{94-y}Au_6Fe_y$ ($y$ = 0.2 to 1.0 at %) specimens in the FQ state. These spectra, as well as the similar spectra obtained for the AR and MS states, were fitted using a single line to represent isolated iron atoms, with the effects of iron clusters being represented by a doublet. Details of spectral fit models for the investigation and analysis of iron clusters and precipitates in similar alloys have already been examined by earlier workers [12–15]. The present straightforward fit model proved to be sufficiently adequate to describe the data accurately for monitoring effects due to changes in the iron concentration and sample state. Earlier models used to describe the Cu–Fe system (e.g. the use of several doublets with different values of quadrupole splittings attributed to iron pairs, triplets and so on [12–15] were also applied, but it was found that either the spectra could not be represented well, or the fit diverged. This is clearly due to the effect of the gold in the alloy (see e.g. [16] for differences in the spectral components of the Cu–Fe and Au–Fe systems).

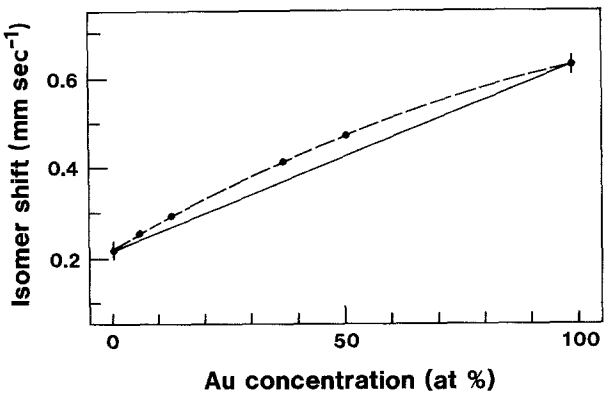


*Figure 2* The isomer shift of $Cu_{99-x}Au_xFe$ alloys as a function of gold concentration.

Consistent with previous investigations of Cu–Fe alloys (e.g. [14]), the present analysis of Cu–Au–Fe alloys showed that the relative contribution of isolated iron atoms, as measured by the fractional area of the single line, decreased with increasing iron concentration, whereas the amount of iron atoms in clusters increased. A slightly enhanced fraction of the single-line spectral component due to isolated iron atoms

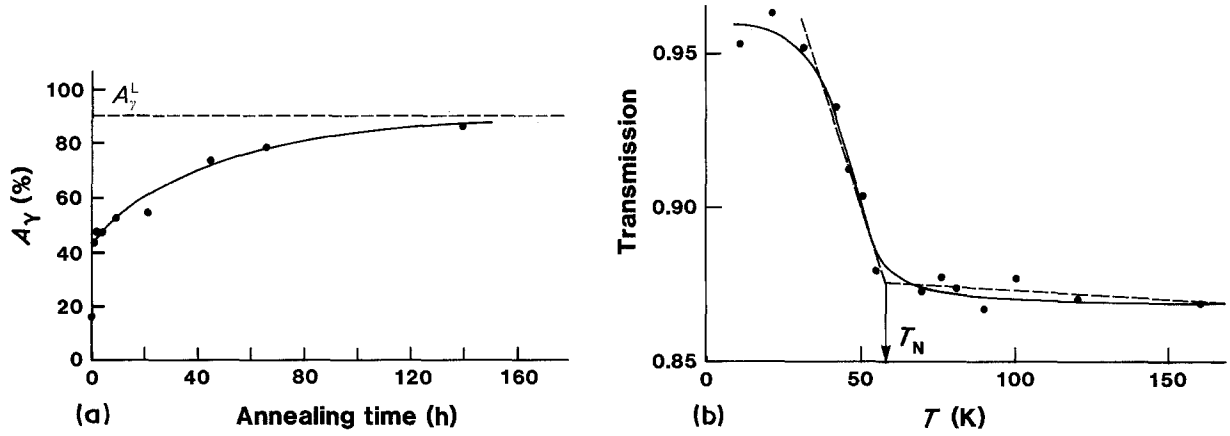


*Figure 4* (a) A graph of $A_\gamma$, the area of the single line used to describe the $\gamma$-Fe component present in the $Cu_{87}Au_{12}Fe$ specimen heat-treated for various times at 410° C (cf. Fig. 3), against annealing time. The exponential growth [20] is shown by the fitted line (see text) with $A_\gamma^L$ indicating the asymptotic limit. (b) The variation of gamma-ray transmission with temperature at constant velocity corresponding to the $\gamma$-Fe resonance for the $Cu_{87}Au_{12}Fe$ specimen heat-treated at 410° C for 139 h. The trend of the data is shown by the full line with the dashed straight lines indicating the value estimated for $T_N$.

was observed in specimens in the AR state, compared with FQ and MS specimens. The general behaviours of isolated iron atoms and clusters in the FQ and MS states are similar, indicating that the rapid quench of the FQ state simulated approximately the equivalent state of atomic disorder obtained in the more rapidly quenched MS state. As in the case of Cu–Fe alloys, the slightly larger fraction of isolated iron atoms in the AR state compared with the FQ and MS states indicates that clusters are to some extent broken up during the cold-rolling process [12].

Fig. 2 shows the isomer shifts (IS) of $Cu_{99-x}Au_xFe$ alloys in the FQ state plotted against $1/a_0^3$ where $a_0$ is the lattice parameter [8] (IS values of the $Cu_{94-y}Au_6Fe_y$ alloys in the three different states were essentially the same). Addition of the relatively large gold atoms to the copper host causes a decrease in the s-electron density at the nucleus and it is clear that atomic volume changes [17] account for almost all of this change in IS with shielding effects (Cu $3d^{10}4s^1$; Au $5d^{10}4s^1$), as expected, causing little or no effect in screening of the charge density at the nucleus. As the isomer shift is proportional to the product of the electron charge density and the relative change of the nuclear radius between excited and ground states (negative for $^{57}Fe$; [18]), this decrease in electron density results in the observed increase of IS with increase in gold concentration. The variation of IS is very similar to the positive deviation from Vegard's law which is observed in the variation of the lattice parameter with gold concentration for the same set of Cu–Au–Fe alloys [8].

Fig. 3 shows the effects of annealing $Cu_{87}Au_{12}Fe$ at 410° C for various times. This temperature was chosen in order to examine the evolution of metastable $\gamma$-Fe precipitates. $\gamma$-Fe in its metastable fcc precipitate stage coherent with its matrix can be readily identified in the spectrum of the 139 h aged sample, e.g. by its IS $\cong -0.07\,\text{mm sec}^{-1}$ (e.g. [7, 19]). The spectra were fitted using a single Lorentzian line to represent the $\gamma$-Fe, with a doublet being used to account for iron atoms in other clustered and surface states. Fig. 4a shows the expected exponential increase of iron atoms in the $\gamma$-Fe state with increasing annealing time, accompanied by the simultaneous decrease of the fraction of iron atoms in other states. The full line shows a fit to the data given by $A_\gamma = a - b\exp(-ct)$ for long-time annealing [20] where $a = 90\%$, $b = 45\%$ and $c = 1/\tau = 1/48\,\text{h}^{-1}$. The rapid increase in $\gamma$-Fe precipitation during the initial stages of heat treatment is probably due to the healing-up of the vacancies produced during the fast quench. Thereafter the precipitation process proceeds rather slowly, with the asymptotic limit of order 90% still not reached after an annealing time of 139 h. It is interesting to note that, despite this long annealing time, no transformation from fcc $\gamma$-Fe to bcc $\alpha$-Fe is found to occur, indicating that the $\gamma$-Fe precipitates have not yet reached the critical size for transformation.

Previous workers [21] have established a relationship between the Néel temperature and particle size for $\gamma$-Fe precipitated in copper. The Néel temperature of the present sample was therefore determined in order to obtain a guide to the particle size and for comparison with the TEM measurements described below. The magnetic ordering temperature was determined using the thermal scanning method [19] in which the absorption of the reasonance line of $\gamma$-Fe is measured as a function of temperature at constant velocity. Fig. 4b shows the change in absorption (or relative transmission) which occurs at the ordering temperature. The 4.2 K spectrum of this sample exhibited a hyperfine splitting of about 1.8 T consistent with typical values observed in antiferromagnetic $\gamma$-Fe precipitated in a copper host (e.g. [7, 19, 21]). The onset of the magnetic hyperfine splitting at the ordering temperature causes a broadening of the unresolved hyperfine pattern and therefore correspondingly an increase in the relative transmission. The thermal scan of Fig. 4b indicates an average Néel temperature of $T_N \cong 60 \pm 2$ K, with the distribution of particle sizes causing the spread in $T_N$ values and the scatter in the curve.

### 3.2. Transmission electron microscopy

Fig. 5 shows dark- and bright-field micrographs of $Cu_{87}Au_{12}Fe$ alloys in the FQ state. Specimens were selected for study in this state as the recrystallization

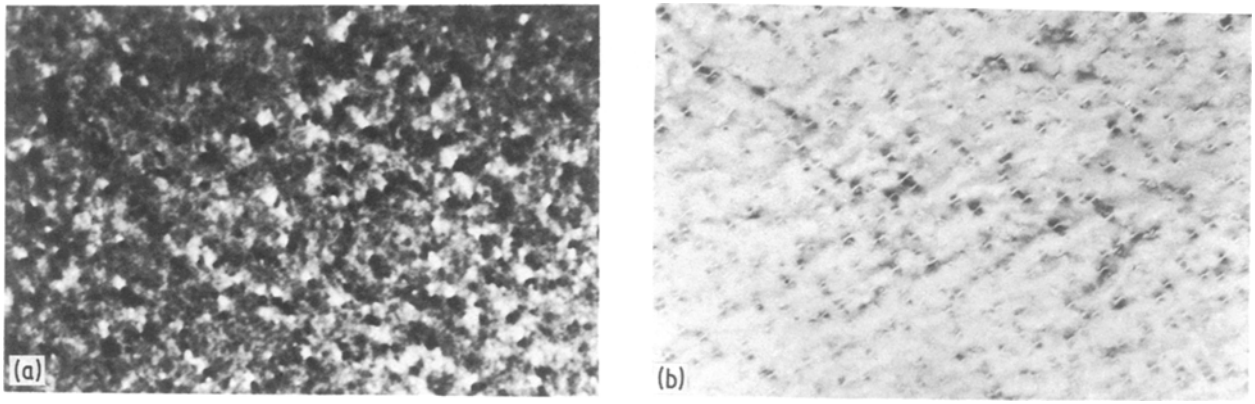


*Figure 5* (a) Dark-field and (b) bright-field micrographs of $Cu_{87}Au_{12}Fe$ specimens: (a) in the FQ state revealing clusters and pre-precipitates as black dots, and (b) in a heat-treated state (410° C, 139 h) revealing $\gamma$-Fe precipitates.

process associated with the heat treatment diminishes the dislocation density. Specimens in the AR state exhibited a very high density of dislocation lines and proved to be unsuitable for measuring the particle sizes of precipitates.

The pronounced black dot pattern of the FQ $Cu_{87}Au_{12}Fe$ specimen (Fig. 5a) may be due either to effects of short-range order in the matrix or to a relatively high density of vacancy clustering associated with the ion-beam etching of the sample thinning technique. The bright-field micrograph of such a sample heat-treated (410° C, 139 h) to produce $\gamma$-iron (Fig. 5b) reveals a change to a strain-field contrast providing evidence consistent with the Mössbauer spectra (Fig. 3) of the existence of fully coherent $\gamma$-Fe precipitates [11, 22–25]. According to Ashby and Brown [22, 23] this contrast is due to elastic strains in the matrix around the precipitates. The criteria for minimal misfit parameters [22, 23, 26] allow the size of the $\gamma$-Fe precipitates to be determined from the strain-field contrast. The misfit parameter $\delta$ is given by the ratio of the room-temperature lattice parameter of the $\gamma$-Fe segregates ($a_0(\gamma\text{-Fe}) = 0.3588\,\text{nm}$) and the matrix ($a_0(Cu_{87}Au_{12}Fe) = 0.36847\,\text{nm}$), yielding $\delta = 0.0259$. With increasing particle size the contrast field increases around the segregates until the misfit is of the order of the Burgers vector $|\boldsymbol{b}| = a\langle 1\,1\,0\rangle/2 = a2^{1/2}/2 \cong 0.26\,\text{nm}$ for the fcc $Cu_{87}Au_{12}Fe$ lattice. The value $(1/\delta)|\boldsymbol{b}| \cong 10\,\text{nm}$ gives the upper limit of the size of the coherent $\gamma$-Fe segregates [22, 23]. In view of this low misfit parameter the mean diameter of the $\gamma$-Fe particles can be extracted directly by measuring the contrasts in Fig. 5b. This yields an average size of about 10 nm for $\gamma$-Fe precipitates in the heat-treated $Cu_{87}Au_{12}Fe$ alloy (410° C, 139 h). By comparison, fully coherent $\gamma$-Fe precipitates of comparable sizes ($\sim 15\,\text{nm}$) are found to develop in the binary Cu–Fe system on annealing at 500° C for the relatively short time of about 5 to 50 min [6]. Further comparison with the Cu–Fe system shows that a Néel temperature $T_N \cong 55\,\text{K}$ is obtained for $\gamma$-Fe precipitates of particle size of order 10 nm, slightly less than the value of $T_N \cong 60\,\text{K}$ obtained in the Cu–Au–Fe system.

## 4. Summary

The precipitation behaviour of pre-precipitates and fully developed coherent fcc $\gamma$-Fe has been investigated in $Cu_{94-y}Au_6Fe_y$ ($y = 0.2$ to 1.0 at %) and $Cu_{87}Au_{12}Fe$ alloys in different metallurgical states. Precipitation generally proceeds in a manner similar to that in the established Cu–Fe system, although slight differences are observed. Dark- and bright-field micrographs show the change in pre-precipitate and particle sizes for the initial and final precipitation states. $\gamma$-Fe precipitates of Néel temperature $T_N \sim 60 \pm 2\,\text{K}$ and particle size of order 10 nm have been obtained in a heat-treated $Cu_{87}Au_{12}Fe$ alloy. The isomer shift is found to vary inversely with the host atomic volume.

## Acknowledgements

We wish to thank members of the Department of Solid State Physics, Australian National University for access to their ribbon-spinning and Mössbauer facilities and particularly Dr. A. Calka for assistance with melt-spinning the samples. We also acknowledge Professor H. Gleiter, Dr. K. Smidoda and Mr M. Schuler for assistance with the transmission electron microscopy measurements as well as useful discussions with Professor K. E. Easterling. This work is supported by grants from the Deutsche Forschungsgemeinschaft and the Australian European Awards Programme.

## References

1. E. OROWAN, "Dislocations in Metals", edited by M. Cohen (Institute of Metals Division, American Institute of Mining and Metallurgical Engineers, New York, 1954) p. 69.
2. R. E. REED-HILL, "Physical Metallurgy Principles" (Van Nostrand, New York, 1964) p. 236.
3. F. S. HAM, *J. Phys. Chem. Solids* **6** (1958) 335.
4. M. HANSEN and K. ANDERKO, "Constitution of Binary Alloys" (McGraw-Hill, New York, 1958) p. 580 and 203.
5. B. WINDOW, *J. Phys. C: Metal Phys. Suppl.* No. 3 (1970) S323.
6. K. EASTERLING and H. M. MIEKK-OJA, *Acta. Metall.* **15** (1967) 1133.
7. S. J. CAMPBELL and P. E. CLARK, *J. Phys. F.* **4** (1974) 1073.
8. D. K-H. FINKLER, A. E. MAURER, S. J. CAMPBELL, T. HECK and U. GONSER, *Physica* **145B** (1989) 335.
9. D. J. BARBER, in Proceedings of 5th European Congress

on Electron Microscopy, Manchester, 1972 (Institute of Physics, London 1972) p. 293.
10. R. E. HURLEY, L. LAURENSON and L. HOLLAND, in Proceedings of 7th International Congress on Electron Microscopy, Grenoble, 1970 edited by P. Favard (Soc. Francaise de Microscopie Electroniques, Paris, 1970) Part 1, p. 299.
11. K. E. EASTERLING, *Acta Polytech. Scand. Chem. Metall. Series* No. 61 (1967) 1.
12. B. WINDOW, *Phil. Mag.* **26** (1972) 681.
13. S. J. CAMPBELL, P. E. CLARK and P. R. LIDDELL, *J. Phys. F.* **2** (1972) L114.
14. S. J. CAMPBELL and T. J. HICKS, *ibid.* **5** (1975) 27.
15. T. J. PANEK and J. KANSY, *ibid.* **12** (1982) 269.
16. G. L. WHITTLE and S. J. CAMPBELL, *J. Mag. Magn. Mater.* **31–34** (1983) 1337.
17. R. INGALLS, F. van der WOUDE and G. A. SAWATZKY, in "Mössbauer Isomer Shifts", edited by G. K. Shenoy and F. E. Wagner (North-Holland, Amsterdam, 1978) p. 361.
18. U. GONSER (ed.), "Mössbauer Spectroscopy", Topics in Applied Physics Vol. 5 (Springer, Berlin, 1975) p. 22.
19. U. GONSER, C. J. MEECHAN, A. H. MUIR and H. WIEDERSICH, *J. Appl. Phys.* **34** (1963) 2373.
20. P. HAASEN, "Physikalische Metallkunde" (Springer, Berlin, 1974) p. 178.
21. D. L. WILLIAMSON, W. KEUNE and U. GONSER, in Proceedings of International Conference on Magnetism, Moscow 1973, Vol. 1 (Nauka, Moscow, 1974) p. 246.
22. M. F. ASHBY and L. M. BROWN, *Phil. Mag.* **8** (1963) 1083.
23. *Idem, ibid.* **8** (1963) 1649.
24. M. RUEHLE, *Phys. Status. Solidi* **19** (1967) 263.
25. M. WILKENS and H. O. K. KIRCHNER, *Phil. Mag.* **A48** (1981) 139.
26. N. F. MOTT and F. R. N. NABARRO, *Proc. Phys. Soc.* **52** (1940) 86.

*Received 3 November 1987*
*and accepted 25 February 1988*